A STUDY ON RECORDING AND REPRODUCTION OF DIGITAL DATA ON AND FROM MAGNETIC DRUM SURFACE

DWIJESH DUTTA MAJUMDAR

INDIAN STATISTICAL INSTITUTE, CALCUTTA-35

ABSTRACT. The basic requirements and role of storage section in all Information Processing System is explained with reference to digital data recording and reproduction on and from magnetic drum surface. A comprehensive theoretical and experimental investigation accompanied by physical interpretations of the process of digital data recording and reproduction on and from ferromagnetic layer surface of Magnetic Drum Memory is presented. The associated boundary value problem has been solved to find the distribution of the fringing field in the ferromagnetic layer and analytic expressions for the output of a write-read system is presented in terms of the basic system parameters. As a result of the investigations basic requirements for achieving high resolution pulse recording on a magnetic surface are shown to be high coercivity, low permeability, rectangular B-H loop characteristics, thin coating, optimum recording current and an optimum pole face configuration for having maximum flux gradient on the surface for a particular head-to-medium separation and coating thickness.

INTRODUCTION

The basic requirements of a storage device or memory system of any of the Information Processing System (IPS) are as follows :-

a) Physical stability of the stored data, so that the information can be retained for an extended period, if desired.

b) Combination of both physical properties of nonvolatility and alterability.

c) Total capacity of the device to hold binary information should be high enough.

d) "Access time" or maximum waiting time for reading from or writing on to a desired address location should be as small as possible.

Using well-known physical principles involved in audio-recording on magnetic surfaces, Digital Information Storage Systems are built (Bigelow, 1948; Booth, 1949; Dutta Majumdar, 1958; Dutta Majumdar, 1961) which satisfies all the above requirements.

In the system under investigation binary information are recorded on a magnetizable surface coated on a rotating nonmagnetic metallic cylinder known as "Magnetic Drum Memory".

2

Pulse recording on magnetic drum surface has attained a unique position, in the field of digital data storage, because both the basic requirements of a binary memory, ability to record two states of a binary digit, and to consult the stored data at anytime are satisfied in this type with simplicity and economy. Theoretical and experimental investigations on optimum design of magnetic drum stores, for serial, serial parallel, or parallel type of digital computers were undertaken by the present author, several aspects of which were published in different technical journals (Dutta Majumdar, 1958, 1959, 1961, 1962). In this paper the mathematics and physics involved in the process of pulse recording and reproduction on and from a moving magnetic surface with the help of a magnetic head is studied. Field configuration in and around the gap of the magnetic head is deduced, computed numerically and plotted, which gives a qualitative insight into the problem of head design. Calculation of the magnetic field in the ferromagnetic layer of the drum in certain cases is presented following a method similar to that of (Karlqvist, 1954), from which variation of the field components with permeability, layer thickness, airgap and other factors involved in the process are studied briefly. Linear boundary value problem for the two-dimensional static field and the one-dimensional transient field has been studied. Pulse frequency has been assumed low enough to neglect eddy current losses in the head and layer that are made of spinel material. The results of some experimental investigations, carried out with a practical magnetic drum storage system, designed and built here, providing reasonable balance between conflicting requirements of access time, storage capacity, reliability, size and cost, are presented and analysed.

Physics involved in the process of magnetic recording in general is rather complicated by the facts that, the particles subjected to the recording field are not of uniform sizes, and the variation of the amplitude of the applied field are different at different depths thereby causing variations in the associated magnetic properties, and once the signal is recorded an interaction occurs between places of different magnetization giving rise to a demagnetization field, and an intricated interdependence of all these and many other parameters. But in saturation type pulse recording the errors involved in the simplifying assumptions made in theoretical deductions are less important, and experimental studies on variation of diferent parameters involved can be made with sufficient accuracy. The present study involving comprehensive theoretical and experimental investigations has provided us a guide to the design of record/reproduce head, and optimization of the whole system for high density storage of digital data. The details of the experimental investigation could not be given here to reduce the size of the paper, only the salient features have been presented.

Principles of magnetic data recording and reproduction.

In digital computers, binary system of notation, where every digit is either a"0" or a "1", is invariably used. And this in magnetic data recording storage

means that the magnetic material on the surface is either saturated in a positive or in a negative sense, or completely unmagnetized. Depending upon this basic fact several methods of recording digits are possible, Return to Zero ($R-Z$), Non-Return to Zero ($N-R-Z$), phase modulation methods etc. $N-R-Z$ method enables a much higher pulse packing density than the other methods maintaining the same degree of reliability. $N-R-Z$ method is being used in the system under investigation.

When the individual writing current pulses are spread out in time or distance, so that they occupy a full bit cell the recording method is called a $N-R-Z$ method. Pulses loose their individuality, and the writing current waveform does not return to zero between successive 1's or successive 0's. Instead, the moving magnetic surface, is continuously magnetized to saturation in one direction or the other with the direction of magnetization being reversed, when a "1" follows a "0", or when a "0" follows a "1". The playback signal using a
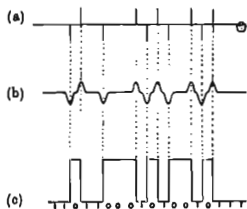

Fig. 1.   (a) Binary current waveform for N. R. Z. Method of recording (b) Actual p.b. signal,
(c) Ideal p.b. signal.

conventional type of head is approximately proportional to the rate of change of flux on the surface. The actual playback signal is shown in fig ((1b). But in ideal case when reading a flux pattern as shown in fig. (1a), the output should be a series of narrow pulses as shown in fig. (1c) corresponding to the flux changes. The original information is extracted from the presence or absence of these pulses. The widening of the output pulses as explained above seriously limits the pulse packing density because the flux changes must be separated sufficiently so that the pulses do not interact.

Magnetic model for write read process using saturation type recording.

The process consists in (1) switching of the state of magnetization of the ferromagnetic surface (Write Process),

(2) self demagnetization of the recorded signal,

(3) playback of the recorded signal (Read process).

The necessary aspects of the problem are to determine the magnetization of the ferromagnetic surface before and after the process of self demagnetization.

Attenuation factors for sinusoidal treatments has been developed and reported in the literature (Wallace, 1951; Begun, 1949; Westmijze, 1953). Now the magnetic model that explains $a-c$ magnetization can be applied with suitable simplifying assumptions, and the recorded pulse magnetization developed in the form of a harmonic series.

The model that explains $a-c$ magnetization is rather simple. In a particle a number of magnetic states are possible, each of which corresponds to a minimum of potential energy and is separated from other minima by potential barriers. Another simplifying assumption that can be made is that these barriers are of equal height. With the application of the magnetic field, the potential energy of those states will be diminished where the direction of the field is more in accord with the direction of the magnetization. Hence the potential barriers will decrease on the one side and will increase on the other side of the potential minimum. For a certain value of the applied field strength the first barriers will have disappeared and the magnetization will jump to a state with lower energy. Since all the barriers were supposed to be of equal height they will be crossed at the same field strength and therefore saturation will be obtained. Reversal of the field effects the saturation in the opposite direction. For an a-c field of sufficient strength the magnetization will alternate between two directions. Now in the process of saturation type digital recording applied magnetic field, of sufficient amplitude to saturate the ferromagnetic surface reverses (switches) its direction of magnetization as steeply as possible, when a "1" follows a "0" or vice-versa. So such a magnetization if developed in the form of a harmonic series, and the attenuation factors developed for sinusoidal treatments referred earlier, can be applied term by term to the total available flux to give the flux passing through the read coil, and by differentiation, the resultant head output voltage is obtained.

Field configuration in and around the gap of the magnetic head.

Before proceeding with the difficult problem of determining the ultimate magnetization of the element on the magnetizable surface in front of the record/read head, we intend to determine the nature of the field configuration in and around the gap. From this investigation we shall be in a position to approximate a potential distribution between the corners of the recording head. The problem has been tackled by Booth and Westmijze. It has been solved in a somewhat different method and is presented here.

At the outset it is assumed that the permeability μ of the head is infinity and that of the layer material is unity.

We approximate a practical head (Fig. 2) such that its left pole piece is bounded by the plane $y = 0$ from $x = -a$ to $x = -l/2$, and by the plane $x = -l/2$. The right pole piece is symmetrical with respect to the plane $x = 0$. This is the case of semi-infinite gap and bears close resemblance to practical heads, but the calculations are rather difficult to carry

out. The other two models, that of infinite gap and thin gap, also treated by Westmijze, are not of much practical use, and so will not be dealt with here.
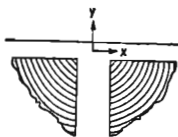

Fig. 2. An approximate practical magnetic head (semi infinite gap).

Looking normal to the gap surface, the gap is infinitely extended in the −ve direction (fig. 2). The assumption that μ of the head material is infinite can be easily approximated as the permeability of the head materials ranges from 10,000 to 100,000 (radiometal, mumetal, permalloy, etc.) and they are not used near the saturation region. The pole surface may then be said to represent a set of magnetic equipotentials.

Supposing there is an one turn coil in the head, and a current I is passed through it, then there will be a magnetic potential difference I between the pole pieces. So the potential function $V(x, y)$ has to satisfy the boundary condition $V = I/2$ and $-I/2$, respectively for the two pole pieces. It is clear from the symmetry that $V(x, y) = 0$ at $x = 0$. We shall apply Schwarz-Christoffel transformation in solving this problems, and then shall numerically compute the equipotential profiles and the lines of forces. (The computation was done in the electronic computer HEC2M).

Equipotential profiles and lines of forces.

We now picture the head on the positive side of the axis in the Z-plane with magnetic pole potentials, $\phi = \pm I/2 = \pm V$.

Application of the Schwarz-Christoffel Transformation gives us the equation from which the transformation of the contour ABCDEF in Z-plane into the W-plane is found. Let length of the head gap to be 2a.

then $$\frac{\partial \phi}{\partial x} = \frac{V}{a} = \frac{\partial \psi}{\partial y} \quad \therefore \quad \psi = \frac{V}{a} y + k.$$

Let $\psi = 0$ at B and E.

From Fig. 3(a) and 3(b)

$$\frac{dz}{dt} = A(t+1)^{\frac{1}{2}}(t-0)(t-1)^{\frac{1}{2}}$$

$$= A\left(\frac{\sqrt{t^2-1}}{t}\right). \qquad \qquad \dots \ (1)$$
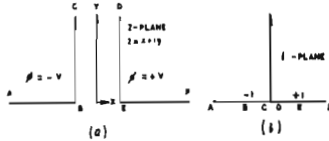
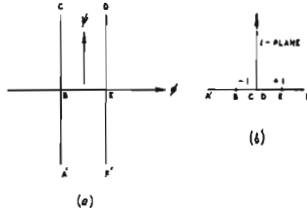*Dwijesh Dutta Majumdar*

Fig. 3. (a) Z-plane, (b) t-plane

Fig. 4. (a) W-plane, (b) t-plane

From Fig. 4(a) and (b)

$$\frac{dW}{dt} = B(t+1)^0 \cdot t^{-1} \cdot (t-1)^0 = \frac{B}{t} \qquad \ldots \ (2)$$

$$\therefore \quad W = B \log t + C.$$

At $\qquad E, t = 1, \quad W = V, \quad \therefore \quad C = V.$

At $\qquad B, t = -1, \quad W = -V$

$$\therefore \quad B = \pm \frac{2V}{i\pi}$$

We take $\qquad W = \frac{2V}{i\pi} \ \log t + V.$

$$= -\frac{2iV}{\pi} \ \log t + V \qquad \ldots \ (3)$$

Since this satisfies the conditions

$$t \to 0, \quad \text{(along real axis)}, \ \psi \to \infty.$$
$$t \to \pm \infty (" \qquad " \qquad ") \ \psi \to \infty$$

From equation (1)

$$Z = A \int \frac{\sqrt{t^2 - 1}}{t} \ dt + D$$

which on integration yields

$$Z = A\left(\sqrt{t^2-1} - \cos^{-1}\frac{1}{t}\right) + D$$

We have $\quad Z = +a \quad$ at $\quad t = +1, \quad \therefore \ D = a$

and $\qquad Z = -a \quad$ at $t = -1, \quad \therefore -a = A\{\cos^{-1}(-1)\} + a$

$$\therefore \ A = \pm \frac{2a}{\pi}.$$

Now we have

$$Z = \frac{2a}{\pi}\left(\sqrt{t^2-1} - \cos^{-1}\frac{1}{t}\right) + a \qquad \ldots \ (4)$$

(valid for $z \to 0$)

From equation (3) we have $\quad t = e^{-\frac{\pi}{2i}\left(\frac{W}{V}-1\right)}$

This when expanded gives

$$t = -i\, e^{-\frac{\pi\psi}{2V}}\left[\cos\frac{\pi\phi}{2V} + i\sin\frac{\pi\phi}{2V}\right]$$

Substituting the value of t in equation (4),

$$Z = \frac{2a}{\pi}\left[\sqrt{-1 - e^{\frac{\pi\psi}{V}}\left\{\cos\frac{\pi\phi}{V} + i\sin\frac{\pi\phi}{V}\right\}}\right.$$

$$\left. -\cos^{-1}\left\{e^{\frac{\pi\psi}{2V}}\left\{i\cos\frac{\pi\phi}{2V} + \sin\frac{\pi\phi}{2V}\right\}\right\}\right] + a. \qquad \ldots \ (5)$$

We take

$$\cos^{-1}\left\{e^{\frac{\pi\psi}{2V}}\sin\frac{\pi\phi}{2V} + ie^{\frac{\pi\psi}{2V}}\cos\frac{\pi\phi}{2V}\right\} = C - iD.$$

This on solution leads to

$$C = \cos^{-1}\left[\frac{1}{\sqrt{2}}\sqrt{\left(e^{\frac{\pi\psi}{V}}+1\right) - e^{\frac{\pi\psi}{2V}}\left\{e^{\frac{\pi\psi}{V}} + e^{\frac{\pi\psi}{V}} + 2\cos\frac{\pi\phi}{V}\right\}^{\frac{1}{2}}}\right] \ \ldots \ (6)$$

$$D = \cos^{-1}\left[\frac{1}{\sqrt{2}}\sqrt{\left(e^{\frac{\pi\psi}{V}}+1\right) + e^{\frac{\pi\psi}{2V}}\left\{e^{\frac{\pi\psi}{V}} + e^{-\frac{\pi\psi}{V}} + 2\cos\frac{\pi\phi}{V}\right\}^{\frac{1}{2}}}\right] \quad \ldots \ (7)$$

Now we take

$$-1 - e^{-\frac{\pi\psi}{A}} \left\{ \cos\frac{\pi\phi}{V} + i \sin\frac{\pi\phi}{V} \right\} = A' - iB' = Re^{i\theta}$$

∴ $A' = R\cos\theta$ and $B' = R\sin\theta.$

$$R = e^{-\frac{\pi\psi}{2V}} \left\{ e^{\frac{\psi\pi}{V}} + e^{-\frac{\pi\psi}{V}} + 2\cos\frac{\pi\phi}{V} \right\} \qquad \dots \ (8)$$

and

$$\tan\theta = -\frac{e^{-\frac{\pi\psi}{V}} \sin\frac{\pi\phi}{V}}{1 + e^{-\frac{\pi\psi}{V}} \cos\frac{\pi\phi}{V}} \qquad \dots \ (9)$$

The equation (5) can now be written as

$$Z = x + iy$$

$$= \frac{2a}{\pi} \left[\sqrt{R}\, e^{-i\theta} - (C - iD) \right] + a$$

$$= \frac{2a}{\pi}(A - C) + a + i(D - B)\frac{2a}{\pi}.$$

where $\sqrt{R}\cos\theta/2 = A$ and $\sqrt{R}\sin\theta/2 = B.$

Therefore,

$$x = \frac{2a}{\pi}(A - C) + a$$
$$\left. \phantom{x = \frac{2a}{\pi}(A - C) + a} \right\} \qquad \dots \ (10)$$
$$y = \frac{2a}{\pi}(D - B)$$

and,

$$A = \sqrt{R}\cos\frac{\theta}{2} = \sqrt{\frac{R}{2}(1 - \cos\theta)}$$
$$\left. \phantom{A = \sqrt{R}} \right\} \qquad \dots \ (11)$$
$$B = \sqrt{R}\sin\frac{\theta}{2} = \sqrt{\frac{R}{2}(1 + \cos\theta)}$$

Substituting the value of $\tan \theta$ from equation (9), we have

$$\cos \theta = \frac{1}{\sqrt{1+\tan^2\theta}}$$

$$= \pm \sqrt{\frac{e^{\pi\phi/V}+e^{-\pi\phi/V}\cos^2\frac{\pi\phi}{V}+2\cos\frac{\pi\phi}{2}}{e^{\pi\phi/V}+e^{-\pi\phi/V}+2\cos\frac{\pi\phi}{V}}} \qquad \ldots \quad (\bar{1}2)$$
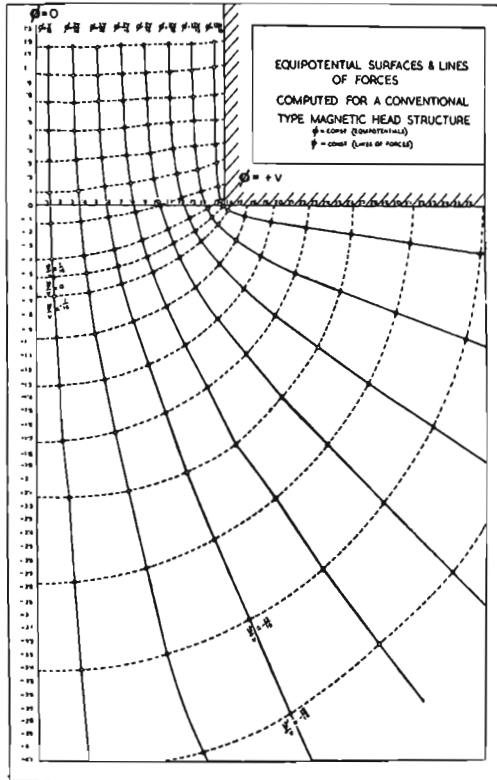

Fig. 5. Equipotential surfaces and lines of forces computed for a conventional type magnetic head structure.

ϕ =const. (equipotentials) ψ =const (lines of forces)

Using equations (6), (7) (10), (11) and (12), the sets of magnetic equipotential profiles and lines of forces are computed and plotted as shown in the Figure 5.

SOLUTION OF BOUNDARY VALUE PROBLEM TO FIND DISTRIBUTION OF FRINGING FIELD OF A SEMI-INFINITE POLE GAP IN FERRO-MAGNETIC LAYER OF A MAGNETIC DRUM

Though the problem is non-linear, the linear case gives a first approximation, which in some cases seems to be satisfactory (Wallace, 1951; Karlqvist, 1954; Booth, 1952). Linear boundary value problem for the two dimensional static field and the one dimensional transient field has been solved and will be dealt with here.

The notations for the physical parameters are :

μ = layer permeability, d = layer thickness, N = half the pole distance, b = head-to-layer distance, B_g = induction in the pole gap measured in volt-sec per sq. meter; $B_g = \mu_0 V/N$, V = magnetic potential of the head, $\mu_0 = 4\pi \times 10^{-7}$ in MKS system.

The investigations on the potential between the corners of the head treated with conformal mapping, shows that the magnetic potential distribution along $y = 0$ can be safely assumed to be linear.

Thus

$$v = -V \qquad x < -N$$
$$v = V \cdot x/N \qquad -N > x > N \qquad \left.\right\} \qquad \ldots \ (13)$$
$$v = +V \qquad x > N$$

So the boundary value problem reduces in finding the magnetic potential $v(x, y)$ in the region $y > 0$, $-\infty < x < \infty$, when the potential along $y = 0$ is prescribed. The magnetizing vector is then,

$$H = -\text{Grad } v(x, y) \qquad \ldots \ (14)$$

The potential satisfies the equation,

$$\frac{\partial}{\partial x} \, \mu \, \frac{\partial V}{\partial x} + \frac{\partial}{\partial y} \mu \, \frac{\partial V}{\partial y} = 0 \qquad \ldots \ (15)$$

We assume μ, the layer permeability as constant, and we get the Laplace's equation:

$$\Delta v = 0, \quad \text{where} \quad \Delta = \frac{\partial^2}{\partial x^2} + \frac{\partial^2}{\partial y^2} \qquad \ldots \ (16)$$

usually the equation (15) is a non-linear equation.

Boundary conditions :

We take $v_1 =$ the potential above the layer $(b-o)$,

$\quad\quad v_2 =$ ''   ''   in   ''   '' $(b+o)$,

$\quad\quad v_3 =$ ''   ''   ''   ''   '' $(c-o)$,

$\quad\quad v_4 =$ ''   ''   below   ''   '' $(c+o)$,

then boundary conditions along $y = b$ and $y = \overset{\omega}{b} + d$ (on the two sides of the layer) are,

$$\frac{\partial V_1}{\partial y} = \mu \, \frac{\partial V_2}{\partial y} \qquad \qquad \ldots \ (17)$$

$$\mu \, \frac{\partial V_3}{\partial y} = \frac{\partial V_4}{\partial y} \qquad \qquad \ldots \ (18)$$

Equations (15) and (16) are elliptic equations.

The non-stationary one-dimensional field can be computed from the equation:

$$\frac{\partial^2 H}{\partial x^2} = \sigma \mu \, \mu_0 \, \frac{\partial H}{\partial t} \qquad \qquad \ldots \ (19)$$

$\sigma =$ conductivity of the layer, $\mu =$ permeability of the layer and is assumed constant.

Idealisation of the problem.

The 1st approximation is to regard the drum surface as plane. The Drum diameter is about 200 mm. and the gap is about .02 mm. The variation of the head to layer distance due to the curvature of the drum surface is less than 10% for the interval $0 < x < 10N$. The factor b/N is usually between 0.5 and 2. The length of the Read/Record head is about 100 to 200 times that of the gap width, and so for all practical purposes, we can assume the head length as infinite. The width of the head is also about 100 times the gap width, and so our two dimensional treatment of the problem will be satisfactory. The permeability of the head is very high, and so the lines of force will leave the head surface nearly perpendicularly. The magnetic potential of the head is therefore assumed constant and is $+Ve$ on the right half and $-Ve$ on the left half of the head. How the pole length influences the field in the layer was investigated by Booth (Booth, 1952); here we shall study the potential between the corners of the head.

The boundary value problem.

We have to find out the potential $v(x, y)$ from the solution of Laplace's equation, subject to the conditions,

$\quad\quad\quad\quad V = 0$ when $y = \infty$ $\quad\quad$ ... (20)

$\quad\quad\quad\quad V = f(x)$ when $y = 0$ $\quad\quad\quad\quad$ (21)

Fourier's Integral solution for this is

$$V = \frac{1}{\pi} \int\limits_0^\infty d\alpha \int\limits_{-\infty}^\infty e^{-\alpha y} f(\lambda) \cos \alpha(\lambda - x) \cdot d\lambda \qquad \cdots \quad (22)$$

Following the same course as in Byerly (*pp.* 78—79),

We obtain

$$v(x, y) = \frac{1}{2b} \sin \frac{\pi y}{b} \int\limits_{-\infty}^\infty f(\lambda) \frac{d\lambda}{\cosh \frac{\pi}{b}(\lambda - x) - \cos \frac{\pi y}{b}} \qquad \cdots \quad (23)$$

And when $b = \infty$ we deduce the formula,

$$v(x, y) = \frac{y}{\pi} \int\limits_{-\infty}^\infty f(\lambda) \frac{d\lambda}{y^2 + (\lambda - x)^2} \qquad \cdots \quad (24)$$

The field for $\mu = \alpha$ is obtained from the equation (23) defined by the equation (13), as :

$$H_y(x, b) = \frac{H_0}{\pi} \log \frac{\cosh \frac{\pi(x+N)}{2b}}{\cosh \frac{\pi(x-N)}{2b}} \qquad \cdots \quad (25)$$

This is not of much practical use. We get the field for the case $\mu = 1$ from the equation (24), which will be of great practical use. The field is always computed from equation (14). The field is given by the equations :

$$H_x(x, y) = -\frac{H_0}{\pi} \left[\tan^{-1} \frac{N+x}{y} + \tan^{-1} \frac{N-x}{y} \right] \qquad \cdots \quad (26)$$

$$H(x, y) = \frac{H_0}{2\pi} \log \frac{y^2 + (N+x)^2}{y^2 + (N-x)^2} \qquad \cdots \quad (27)$$

In the above equations we have the field given explicitly as simple functions of $x + y$, and it is easy to compute actual field. The approximation is satisfactory upto y greater than $0.5N$. The pole gap field intensity H_0 is estimated from a magneto motive force reluctance relationship, where the reluctance of the head core is piecewise calculated. We have

$$H_0 = \frac{4\pi n_1 i}{g_1 \left[1 + \frac{R_p}{R_{g1}} \right]} \qquad \cdots \quad (28)$$

where R_p = reluctance of the head core, R_{g1} = Reluctance of the head pole gap, n_1 is the number of turns on the write coil and

$$\frac{R_p}{R_{g1}} = \frac{A_{g1}}{g_1}\left[\frac{g_2}{A_{g2}} + \sum_{i=1}^{T}\frac{li}{\mu_1 \bar{A}_{p1}}\right] \qquad \dots (29)$$

g_1 = length of pole gap in the write read head ($cm.$),

g_2 = average length of the rear gap (cm),

A_{g1} = area of the pole gap (cm^2), A_{g2} = area of the rear gap (cm^2),

μ_1 = initial permeability of the head core material at the frequency of operation.
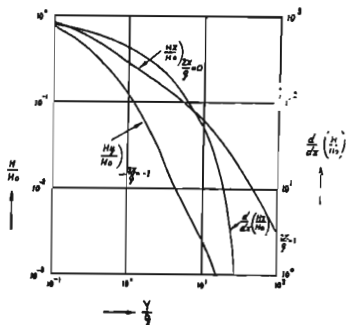
Fig. 6.   Fringing field components H_x, H_y, and the gradient $\frac{\delta H_x}{\delta x}$,

The validity of the above equations was checked by Kostyshin and Roshon ((Kostyshin and Roshon 1959) with the help of a Hall-probe, the vertical component of the fringing field of a magnetic recording head with a .001 inch pole gap was mapped.   The observed and calculated fields agreed to within 4%.

Equations (26) and (27) in terms of the above parameters can be written as

$$H_x(x, y) = -\frac{H_0}{\pi}\left\{\tan^{-1}\left[\frac{1 + \frac{2x}{g_1}}{\frac{2y}{g_1}}\right] + \tan^{-1}\left[\frac{1 - \frac{2x}{g_1}}{\frac{2y}{g_1}}\right]\right\} \qquad \dots (30)$$

$$H_y(x, y) = \frac{H_0}{\pi}\left\{\frac{\left(\frac{2y}{g_1}\right)^2 + \left(1 + \frac{2x}{g_1}\right)^2}{\left(\frac{2y}{g_1}\right)^2 + \left(1 - \frac{2x}{g_1}\right)^2}\right\} \qquad \dots (31)$$

Maximum values of the fringing field components H_x, H_y, and the gradient $\frac{\partial H_x}{\partial x}$ at the point of inflection of the curve are shown in the Fig. 6.

The point of inflexion of H_z and the max^m value of H_y are assumed to occur at $x_1 = \pm g_1/2$, for all values of μ.

The analytical expressions for other two cases, μ greater than 1 but infinite layer thickness and μ greater than 1 and finite layer thickness can be deduced using Fourier's transform method, but for all practical purposes expressions (26) and (27) or (30) and (31) offer very good approximation. (We are using spinel material of very low μ as our ferromagnetic layer).

It is seen that at a distance greater than one tenth of the pole gap, the intensity of the longitudinal (X) component is always greater than the vertical (Y) component. For a typical recording head at a distance equal to the pole gap the intensities of the longitudinal (X) and the vertical (Y) field components may be of the order of 1200 and 700 oersteds respectively. The 1200 oersteds field is sufficient to saturate any of the commonly used storage media in the longitudinal direction. Moreover, because of the shearing of the loop (Began, S. J.) in the vertical direction due to adverse demagnetization conditions, the 700 oersted
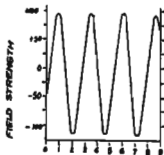
Direction of recording (inches $\times 10^{-3}$).

Fig. 7. Magnetic field strength normal to oxide recording media.
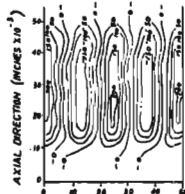
Direction of recording (inches $\times 10^{-3}$).

Fig. 8. Distribution of Magnetic field strength normal to the recording media, signal array continuous series of "ones". Isobars are in oersteds.

field is insufficient to saturate the medium in the vertical direction. So we take it for granted that the magnetization is predominantly of longitudinal nature. This statement was made by the author in a note presented to the Roorki Session of the Indian Science Congress (Dutta Majumdar, 1958) and has been demonstrated by Kostyshin and others (Kostyshin, Roshon etc., 1959) by mapping the fringing fields of signals stored on oxide and on nickel cobalt plated surfaces with a Hall probe and is reproduced here (Fig. 7 and 8). Before going into the more rigorous harmonic analysis and other things, we would like to show how most of the engineering design conditions are derived from the equations (26) and (27).

From (26) and (27) we can compute longitudinal and vertical components of magnetic flux vectors in the media as follows (Fig. 9) :
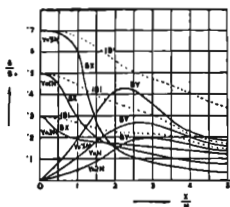
Fig. 9. Graphical plots of equations 32, 33, and 34.

We have

$$B_x = -\frac{B_0}{\pi}\left[\tan^{-1}\frac{N+X}{Y}+\tan^{-1}\frac{N-X}{Y}\right] \qquad \ldots \text{(32)}$$

$$B_y = -\frac{B_0}{2\pi}\left[\log\frac{Y^2+(N-X)^2}{Y^2+(N+X)^2}\right] \qquad \ldots \text{(33)}$$

$$|B| = \sqrt{B^2_x+B_y^2} \qquad \ldots \text{(34)}$$

COMPUTATION OF PLAYBACK VOLTAGE PULSE FROM EQUATION (32)

Considering the idealised play back head to be a semi infinite block of high permeability material with the flat face at a distance b above the recording surface, the *P. B.* signal will be proportional to the rate of change of the X-component of the flux.

Using the method of images, the value of the flux density in the head can be shown to be the same as though the head filled all of space and the intensity of magnetization in the recording medium were $\dfrac{2\mu}{\mu+1}$ times the value actually present.

So,

$$B_x = \frac{2\mu B_0}{\pi(\mu+1)}\left[\tan^{-1}\frac{N+X}{Y}+\tan^{-1}\frac{N-X}{Y}\right] \qquad \ldots \text{(35)}$$

If δ is the thickness of the medium the total flux per unit width will be

$$\phi_x = \int_{b+\delta/2}^{\infty} B_x dy \qquad \ldots \text{(36)}$$

The output voltage will be proportional to the rate of change of ϕ_x; therefore,

$$e(x) = C\frac{d\phi_x}{dt} = C\cdot\frac{dx}{dt} \cdot \frac{d\phi_x}{dx} \cdot = v\cdot C\,\frac{d}{dx} \int\limits_{b+\delta/2}^{\infty} B_x dy$$

$$= v\cdot C \int\limits_{b+\delta/2}^{\infty} \frac{d}{dx}\, B_x dy \qquad \ldots \text{(37)}$$

$$e(x) = \frac{2\mu v e B_0}{\pi(\mu+1)} \int\limits_{b+\delta/2}^{\infty} \left[\frac{y}{y^2+(N+x)^2} - \frac{y}{y^2+(N-x)^2} \right] dy.$$

$$= \frac{\mu v C B_0}{\pi(\mu+1)} \left[\log \frac{y^2+(N+x)^2}{y^2+(N-x)^2} \right]_{b+\delta/2}^{\alpha}$$

$$= \frac{\mu v C B_0}{\pi(\mu+1)} \cdot \log \left[\frac{\left(b+\dfrac{\delta}{2}\right)^2+(N-x)^2}{\left(b+\dfrac{\delta}{2}\right)^2+(N+x)^2} \right] \qquad \ldots \text{(38)}$$

where $C =$ constant of proportionality and $V =$ velocity of the surface. The equation (38) if slightly modified as :

$$e(x) = \frac{\mu v C B_0}{\pi(\mu+1)} \, \text{Log}\left[\frac{(b+\delta/2-a)^2+(N-x)^2}{(b+\delta/2-a)^2+(N+x)^2} \right] \qquad \ldots \text{(39)}$$

where 'a' is greater than 'O' and is a recording constant which incorporates the magnetic properties of the medium. The above expression relates the playback voltage "e" from an ideal head with different physical parameters. These and their graphical plots can be used for design purposes. If the value of a' is determined indirectly, the maximum pulse amplitude and the pulse width at a certain clipping level can be determined.

Demagnetisation curve of layer material.

The portion of the hysteresis loop that lies in the second quadrant between residual induction, Br, and coercive force H_s, is called demagnetization curve. The quantities most used in evaluating the quality of materials are H_s, B_r, and the products H_s B_r, $(BH)_m$, the latter being the maximum product of B and H for points on the demagnetization curve (-ve sign omitted). A given value of magnetic material will produce highest field in a given air space when the induction

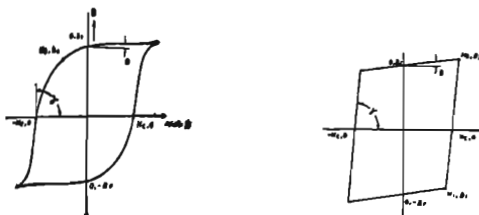B in the material is that for which the energy product BH is a maximum (Evershed, 1958).

Fig. 10. (a) A hysteresis loop, demagnetization curve approximated to a rectangular hyperbola,

(b) hysteresis loop linearized to a parallelogram.

As an empirical mathematical relation the demagnetization curve can be simulated by a rectangular hyperbola (Bozorth, 1951) defined by three points $B_r(H = 0)$, (B_a, H_a), $-H_s(B = 0)$ as shown in Fig. (10a)

The shape of the demagnetization curve between B_r and H_s is fixed by what is often called the fullness factor, defined by

$$\gamma = \frac{(BH)_m}{B_r H_s} \qquad \cdots \ (40)$$

and the squareness factor, S, defined retentively by the ratio of the B_r to the asymptotic magnetization predicted by the hyperbola and is given by the equation

$$S = \frac{m+h-1}{mh} \qquad \cdots \ (41)$$

where

$$m = \frac{B_a}{B_r} \text{ , and } h = -\frac{H_a}{H_s} \text{ ,}$$

S is related to γ by

$$S = 1-(\gamma-1)^2 \qquad \cdots \ (42)$$

Using the general expression for a rectangular hyperbola

$$(x-x_0)(y-y_0) = C_0^2 \qquad \cdots \ (43)$$

and making substitutions and simplifications, the second quadrant of the hysteresis loop is given by the equation :

$$B = \frac{B_r(1-H/H_s)}{1-S(H/H_s)} \qquad \cdots \ (44)$$

4

The reversible permeability μ_p of the storage medium, considered constant (Westmijze, 1953), is defined by the slope of the hyperbola at the point $(0, B_r)$, where

$$\mu_2 = 1 + \tan\theta \qquad \qquad \cdots \ (45)$$

and

$$\tan\theta = \frac{B_r}{H_s}(1-S) \qquad \qquad \cdots \ (46)$$

So it is seen that the reversible permeability μ_2, is dependent on the squarness factor S. The slope of the hyperbola at the point $(H_c, 0)$ is given by the equation :

$$\tan\alpha = \frac{B_r}{H_c}\left(\frac{1}{1-S}\right) \qquad \qquad \cdots \ (47)$$

Write process : For the write process only, we linearize the entire hysteresis loop to a parallelogram (fig. 10b), then the field intensities at the beginning and at the end are given by the equations :

$$H_1 = \frac{H_s}{2-S} \ , \quad H_2 = \frac{H_c}{S} \qquad \qquad \cdots \ (48)$$

From the mathematical and physical analysis earlier we assumed the magnetization of the medium as predominantly longitudinal. In the mechanics of NRZ recording, the longitudinal component of magnetization may be represented by a trapozoid.   The transition length of magnetization (Fig. 11) is equal to the average dynamic transition length b_d with a lower limit imposed by the static transition length b_s.
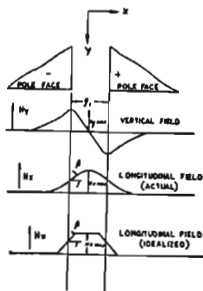

Fig. 11. Longitudinal component approximated to a trapezoid

The static transition length b_s is determined by the shape of the hysteresis loop of the layer material and the pattern of the fringing field at the pole gap.

And the dynamic transition length is determined by the time constants of the write circuitry, the relative velocity of the head and storage medium, and the reluctance of the head core.
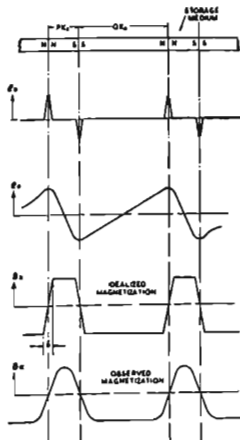

Fig. 12.   A typical signal array where a succession of ones are separated by p and o 'bit' leangths.

For the typical signal array (Fig. 12) where a succession of ones are separated by p and q bit length, the resultant magnetization is described by the Fourier Series (Kostyshin, 1961) :*

$$B = \sum_{n-1}^{\infty} B_0 \left\{ \frac{p-q}{p+q} + \frac{4}{n\pi} \cdot \sin \frac{n\pi}{1 + \frac{q}{p}} \cdot \frac{\sin \frac{n\pi b}{(p+q)k_0}}{\frac{n\pi b}{(p+q)K_0}} \cdot \cos \frac{2n\pi x}{(p+q)K_0} \right\} \dots (49)$$

The corresponding harmonic wave length and the equivalent harmonic frequency are defined by the equations :

$$\lambda_n = \frac{(p+q)K_0}{n} \qquad\qquad \dots (50)$$

$$f_n = \frac{nV}{(p+q)K_0} \qquad\qquad \dots (51)$$

Self Demagnetisation of the recorded signal.

As soon as the recording head is removed from the vicinity of the recorded cell, the boundary conditions change resulting in a demagnetizing field H_d and a quiscent magnetization B_d. During reading operation, the boundary conditions similar to those of Write process are re-established, and ideally at least the demagnetizing field is reduced to zero, and the resulting magnetization B_n (the initial magnetization considered for the Read process) is slightly lower than the retentivity of the storage medium. This is due to the nonlinear character of the hysteris loop and the constancy of the reversible permeability of the medium.
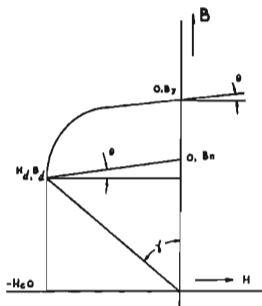

Fig. 13. Demagnetization curve.

It is a standard practice to define a demagnetization factor (Westmijze, 1953) as

$$D_n = \tan \gamma = -\frac{H_d}{B_d} \qquad \qquad \dots \ (52)$$

B_n is then determined by the values of H_d and B_d and by the angle defined by the reversible permeability of the storage medium as shown in Fig. 13 (Bozorth, 1951)

Assuming the magnetization to be constant throughout the depth the average demagnetization factor is defined by the equation :

$$\bar{D}_n = \frac{\displaystyle\int_{b_1}^{b_1+d} D_n dy}{\displaystyle\int_{b_1}^{b_1+d} dy} \qquad \qquad \dots \ (53)$$

b_1 = head to storage medium distance during write process and d = layer thickness. D_n is determined from an expression for H_d and B_d similar to that given by West-mijze (Westmijze, 1953) which need not be treated here.

The resultant initial harmonic magnetization after self-demagnetization is given by the equation (Kostyshyn, 1961) :

$$B_n = H_s \left\{ \left[\frac{1 + \bar{D}_n(\mu_s - 1)}{2S\bar{D}_n} \right] \left[1 + \bar{D}_n \frac{B_r}{H_s} - \right. \right.$$

$$\left. \left. \left(1 + D_n \frac{B_r}{H_s} \right) \times \left(2 - 4S + \bar{D}_n \frac{B_r}{H_s} \right)^{\frac{1}{2}} \right] \right\} \qquad \ldots \text{(54)}$$

Process of play back :

The next problem obviously is to determine the total quantity of fringing flux of the stored bit in the cell that passes through the read coil when there is a reading operation. Westmijze (Westmijze, 1953) has described the loss term, assuming of course the head permeability as infinity and a non-zero head to layer spacing due to physical dimensions of the head to medium gap, the thickness of the medium and the reversible permeability of the medium. Total flux through the head coil can thus be determined which on differentiation gives the output voltage of the read coil. By considering an equivalent read circuit, the loading effect of the amplifier, the line and the stray capacitance of the read coil can be taken account of. Following the above logic, the expression for the head output voltage, for the signal array described by equation (49), is given by the equation :

$$E_0 = \sum_{n=1} X_n Y_n C_n E_n L_n B_n \{4N_2 W V\} \sin \frac{n\pi}{1 + q/p}$$

$$\sin \frac{\pi}{\lambda n} \left\{ X + \frac{g_1}{2} \right\} . 10^{-8} \text{ volt.} \qquad \ldots \text{(55)}$$

where,

$$X_n = \frac{1}{1 + \frac{R_p}{R_{g_1}}} \quad R_p = \text{reluctance of the head core} \qquad \ldots \text{(56)}$$

$$R_{g_1} = \text{reluctance of the head pole gap}$$

$$Y_n = \frac{\sin \frac{\pi g_1}{\lambda_n}}{\frac{\pi g_1}{\lambda_n}} \qquad \ldots \text{(57)}$$

$$C_n = \frac{1}{n\pi} \left\{ \frac{\tanh\frac{\pi d}{\lambda_n}}{\cosh\frac{\pi b}{\lambda_n}} \cdot \frac{1 + \frac{1}{\mu_2} \cdot \tanh\frac{\pi d}{2\lambda_n}}{1 + \tanh\frac{\pi b_2}{\lambda_n} + \tanh\frac{\pi d}{\lambda_n}\left[\frac{1}{\mu_2} + \mu_2 \tanh\frac{\pi b}{\lambda_n}\right]} \right\} \qquad \dots \quad (58)$$

$$E_n = \frac{\sin\frac{\pi b}{\lambda_n}}{\frac{\pi b}{\lambda_n}}, \qquad \dots \quad (59)$$

$$L_n = \frac{1}{1 + \frac{Z_1}{Z_n}} \qquad \dots \quad (60)$$

N_2 = No. of turns on read coil.

W = width of the head at pole tips (cm.).

V = relative velocity of head and storage medium (cm. per Sec.).

Z_1 = Load impedance of the read network (ohm).

Z_n = equivalent impedance of the read head (ohm).

The reluctance ratio R_g/R_{g1} is given in equation (29), from which X_a is known and the expression for B_n is given by equation (54). The above equations can be programmed for any Electronic Computer and can be applied to various head-recording media systems, and it is possible to study on an analytic basis the effect of varying single parameters of a system.

The case of one dimensional transient field.

In the ferromagnetic layer of a DRUM MEMORY switching the state of magnetization of the specified region on the memory drum surface is accomplished by reversing the direction of an electric current in the write coil of the magnetic recording head. In order to study the transient field associated with this phenomena, it can be assumed that a polarised electro-magnetic wave with the components H_x and E_z comes perpendicular to the ferromagnetic layer.

The electro-magnetic field must satisfy the Maxwell's fundamental equations, and so the corresponding differential equation can be derived from them.

We assume μ = permeability of the layer

$\qquad K$ = constant

$\qquad \sigma$ = conductivity of the layer (1/ohm−meter).

$\qquad \mu_0 = 4\pi 10^{-7}$ in MKS system = 1.257×10^{-6} (henry/meter)

B = electric intensity (volts/meter)

B = magnetic Induction (weber/meter)

D = electric displacement (coloumbs/meter^2)

H = magnetic intensity (amperes/meter)
J = current, density (amperes/meter²)
ρ = charge density (coloumbs/meter³)

Maxwells' Equations are :

$$\left. \begin{array}{ll} \Delta \times E = \quad -\dfrac{\partial B}{\partial t} & \quad \Delta \cdot B = 0 \\[3mm] \Delta \times H = J + \dfrac{\partial D}{\partial t} & \quad \Delta \cdot D = \rho \end{array} \right\} \qquad \ldots (61)$$

In a homogeneous isotropic medium we have the additional relations

$$D = KE, \quad B = \mu H, \quad \text{and} \quad J = \sigma E.$$

From the above relations we have,

$$\left. \begin{array}{l} \Delta \times E = \mu \dfrac{\partial H}{\partial t} \\[3mm] \Delta \times H = \sigma E \end{array} \right\} \qquad \ldots (62)$$

We have $H_y = H_z = 0$, and $E_x = E_y = 0$,

$$\Delta \times H = \begin{vmatrix} i & j & K \\[2mm] \dfrac{\partial}{\partial x} & \dfrac{\partial}{\partial y} & \dfrac{\partial}{\partial z} \\[2mm] H_n & 0 & 0 \end{vmatrix}$$

$$\therefore \quad \frac{\partial H_x}{\partial z} = 0, \quad K \frac{\partial H_x}{\partial y} = K \sigma E_z.$$

And

$$\Delta \times E = \begin{vmatrix} i & j & K \\[2mm] \dfrac{\partial}{\partial x} & \dfrac{\partial}{\partial y} & \dfrac{\partial}{\partial z} \\[2mm] 0 & 0 & E \end{vmatrix}$$

$$= i \frac{\partial E_z}{\partial y} - j \frac{\partial E_z}{\partial x}$$

$$\text{but } \frac{\partial E_z}{\partial x} = 0,$$

$$\therefore \qquad \frac{\partial H_z}{\partial y} = \sigma E_z$$

and
$$\frac{\partial E_z}{\partial y} = \mu \ \frac{\partial H_s}{\partial t}$$

Therefore,

$$\frac{\partial^2 H_s}{\partial y^2} = \sigma \ \frac{\partial E_z}{\partial y} \ = \mu\sigma \frac{\partial H_z}{\partial t}$$

In rationalised M.K.S. system

$$\frac{\partial^2 H_z}{\partial y^2} = \sigma\mu \ \mu_0 \frac{\partial H_z}{\partial t} \qquad \qquad \dots \ (63)$$

The non-stationary one dimensional field can be computed from equation (63) which is a parabolic differential equation and will be solved using Laplace's transforms.

The equation (63) is to be solved for infinite layer and for finite layer.

Infinite layer : The wave is applied suddenly at $t = 0$, and the air gap b is assumed to be zero. The initial value problem is :

$$H_{(0,t)} = H_0, \quad H_{(\infty,t)} = 0, \quad H_{(y,0)} = 0.$$

(X—coordinate has been replaced by y)

[Laplace transform $f(p)$ of the function $F(t)$ is defined by

$$f(p) = \int_0^\infty e^{-pt} F(t) dt]$$

Then the Laplace transform of the equation (63) can be written as

$$h = \frac{H_0}{p} \ e^{-ky\sqrt{p}}, \ K^2 = \sigma\mu \ \mu_0.$$

The corresponding time function is

$$H_{y,t} = H_0 \ \text{erfc.} \ y\sqrt{\frac{\sigma\mu\mu_0}{4t}} \qquad \qquad \dots \ (64)$$

is defined by the equation

$$erfx = 1 - erfc \ x = \frac{2}{\sqrt{\pi}} \int_0^x e^{-t^2} dt.$$

Finite layer thickness : While considering this case we have to assume that the Z-component of electric intensity, E_z, is continuous on the other side of the

layer, that is, at the point $y = d$, then if σ_1 and σ_2 represent conductivities of the layer material and drum—material respectively

$$\text{Lim} \cdot \sigma_2 \, \frac{\partial H}{\partial y} = \text{Lim} \cdot \sigma_1 \, \frac{\partial H}{\partial y} \, .$$

$$y \to d - 0 \qquad\qquad y \to d + 0$$

The conductivity of the ferromagnetic layer material σ_1 can be considered as zero in comparison with that of the drum material (usually brass).

We have the Laplace transform

$$h = H_0 \frac{e^{-(y-d)k\sqrt{p}}}{\cosh Kd\sqrt{p}}$$

and the corresponding time function is,

$$H_{(d,t)} = 2H_0 \sum_{n=0}^{\infty} (-1)^n \, erfc \left[(2n+1)d\sqrt{\frac{\sigma \mu \mu_0}{4t}} \right] \qquad \ldots (65)$$

$$\to \frac{d\sqrt{\sigma\mu\mu_0}}{2\sqrt{t}}$$
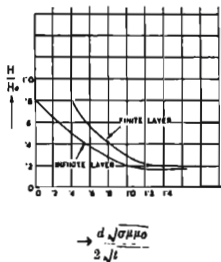
Fig. 14. Magnetic field in transient case.

From these two cases one can compute the transient time of the layer material, and their dependence on σ, μ, and d.

EXPERIMENTAL INVESTIGATION

In order to carry out a thorough investigation on the problems and limitations associated with arriving at a wholly rational design of a magnetic drum store, an experimental magnetic drum unit was designed, constructed, coated, and finished by ourselves in our Laboratory. The engineering description, the drum coating technique, and its digital data recording and reproduction techniques were described earlier (Dutta Majumdar, 1961).

For experimental purposes, factors that affect pulse resolution should be broadly classified as (a) frequency dependent factors and (b) wavelength dependent factors. Frequency dependent factors in pulse recording are (1) recording current and flux rise time, (2) frequency response of the amplifiers, (3) frequency response of the magnetic heads. It is obvious that the frequency dependent factors can be made very negligible. Wave length dependent factors are considered to be more basic with respect to the recording and reading out of the pulses and here the results of the theoretical investigations presented earlier are of great help. In our magnetic model of Write-Read process using saturation type recording we have explained that the process consists in (1) switching of the state of magnetization, (2) self-demagnetization of the recorded signal and (3) playback of the recorded signal. It has been explained in an earlier publication (Dutta Majumdar, 1959) how the variables involved in the process are interrelated in a complex manner. For the clarity of the concept the variable factors can be combined and grouped as (1) Recording procecess limitations and (2) Playback process limitations. The limitations due to magnetic characteristics of the layer surface are of course, involved in both.

RECORDING PROCESS LIMITATION

Several important limitations of recording process are associated with what is known as Record-Head Trailing Effect, which is commonly defined as the demagnetization of the surface still within the field of the head as it changes polarity.
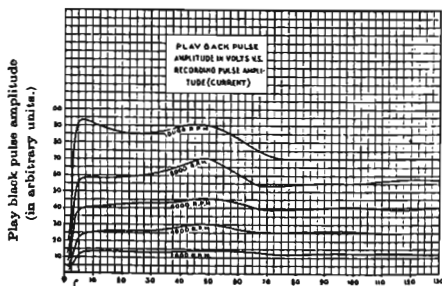

Fig. 15. Variation of P.B. Pulse amplitude (volts) with recording pulse amplitude (current).

In Fig. 15 the variation of P.B. pulse amplitude with recording pulse amplitude is plotted. If the field gradient across the record head had no influence on the flux pattern, one would expect the pulse width and amplitude to remain constant after saturation. But it is seen that they are dependent on recording current. The increase in pulse width and decrease in amplitude may be attributed to the

"record-head trailing effect." At the moment of flux reversal in the head, all particles under the trailing pole face are magnetized to a varying degree dependent on the gradient across the head. The actual field pattern in the coating will
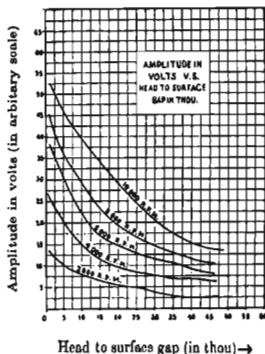

Head to surface gap (in thou)→
Fig. 16. Variation of P.B. Pulse amplitude with head-to-surface gap (in thou.).
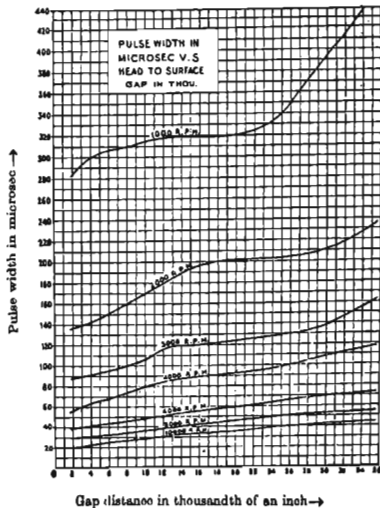
Gap distance in thousandth of an inch→
Fig. 17. Variation of P.B. pulse width in microsecond with head-to-surface gap (in thou).

depend on the permeability of the material saturated to a constant value at distances from the gap. This record head trailing effect is dependent on the *B—H* characteristics of the medium, recording current, coating thickness, head to medium separation and gap width of the record head.

In Figs. 16 and 17 variation of P.B. pulse amplitude and width with Head to Surface gap are plotted for different speeds. In amplitude versus head to surface gap curves it is seen that at higher speeds it tends to become linear. In Fig. 17 it is seen that the pulse width increases with gap distance, at lower speeds the rate of increase is sharper than at higher speeds. It is seen that at 8000 r.p.m. and above, the P.B. pulse amplitude is much less affected by gap variation.
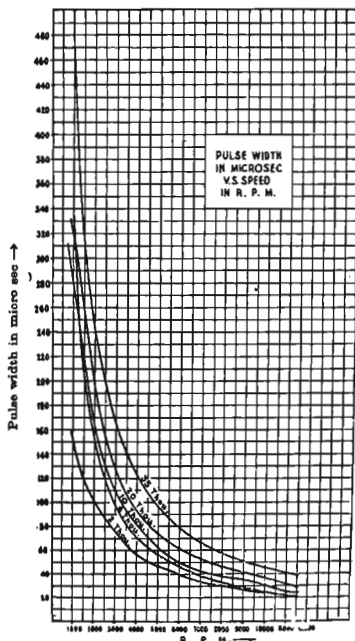

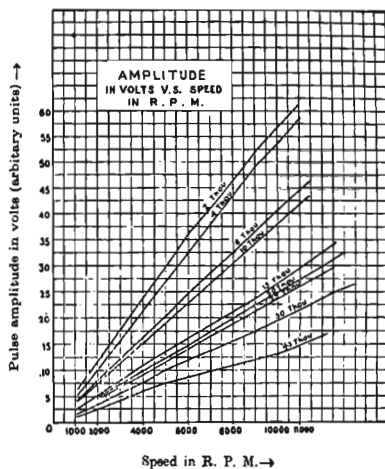Fig. 18. Variation of P.B. pulse width in microsec. with rotational speed in r.p.m.

Speed in R. P. M.→

Fig. 19.   Variation of P.B. pulse amplitude with rotational speed in r.p.m.
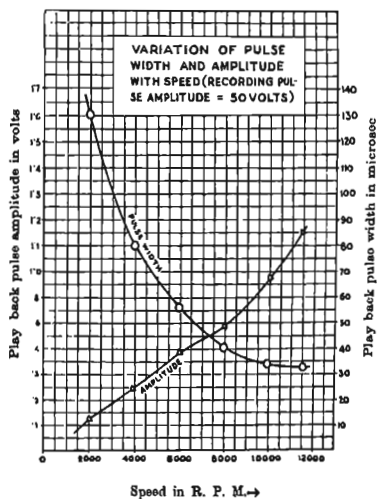

Speed in R. P. M.→

Fig. 20.   Variation of P.B. pulse amplitude and width, with speed in r.p.m. (for a constant recording pulse amplitude).

Pulse width in microsecond versus rotational speed in r.p.m. is plotted in Fig. 18. The curves seem to approximate rectangular hyperbola. Here also it is seen that the affect of speed variation on playback pulse width is much less affected at speed above 8000 r.p.m. In Fig. 19 and 20 where variation of pulse width and amplitude with rotational speed is plotted, the amplitude is seem to rise linearly with speed.

Effect of recording mmf.

The position of maximum flux gradient is the effective recording point, which will depend on the magnetic medium and the recording field strength. We can see it from our theoretical results that the relative distribution of the horizontal and vertical components of the magnetization will depend on the recording field strength and the coating thickness. It has been observed experimentally that a current greater than that required to saturate the surface results in reduction in amplitude and increase in pulse width and consequent loss of resolution. It has been shown earlier in connection with equations (30) and (31) that the longitudinal component is responsible for recording. But if the recording current is increased beyond the saturation current the vertical component becomes predominant, which results in a shift of the effective recording point further away from the centre of the gap, and increases the total distance over which the flux is changing, which obviously results in the increase of pulse width and loss of resolution.

Effect of recording head gap width.

This effect is same as that of the effect of the trailing field gradient as explained earlier. If the gap width is very small, the field gradient will be greater at the pole face surface which will enable us to use a very thin magnetic coating which is desirable from many other consideration. Naturally for thick coatings a wider gap will be desirable to set up a sufficiently strong field to saturate those particles some distance from the pole face. In a nutshell the optimum record head gap will depend on the coating thickness, the B-H characteristics of the layer surface and the separation between the record head and layer surface.

Effect of separation between record head and layer surface :

With increase in separation the layer surface is subject to a diminished recording field gradient, which will widen the flux distribution resulting in the loss of resolution. This loss can be minimised by using a coating with a rectangular B—H characteristics, and by designing a record head that gives maximum field gradient for the particular separation being used.

Effect of magnetic characteristics of the coating material :

Earlier we have tried to explain, on theoretical grounds, the demagnetization curve of the layer material, (equations 40 through 47) and, self-Demagnetization of the recordedsignal (equations 52, 53, 54) Now we apply the term "self-

demagnetization effect" to pulse widening caused by the field within the coating. The field in the coating due to the volume element dv will be $dH = \dfrac{Div\ I\ dv}{r^2}$ where I is the intensity of magnetization, Div I is the "volume density of magnetic charge" and r is the distance from the volume element dv to the point (x, y, z) in the coating. The total field at (x, y, z) will be

$$H = \int \frac{Div\ I\ dv}{r^2} \qquad \ldots \ (66)$$

This field within the coating will act on the particles and tend to reorient the particles and thereby reduce the resolution. This effect can be reduced by using a coating material with high coercivity to remenance ratio which will minimize reorientation of particles, and having a rectangular *B-H* loop characteristics. The demagnetizing field is less with thin coating than with thick coating. Thus from all considerations a considerable improvement w.r.t. resolution is achieved with nearly rectangular hysteresis loop material and a thin coating.
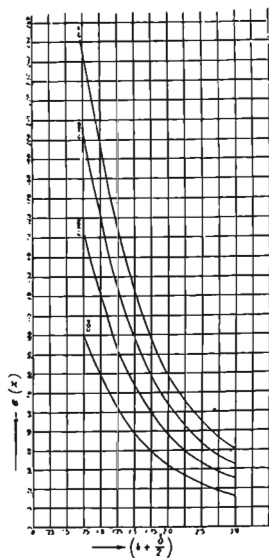

Fig. 21. Computation of P.B. voltage from equation (38) for different physical parameters.

PLAYBACK PROCESS LIMITATIONS

An expression was derived earlier (equation 38), showing how the P.B. signal characteristics depend on coating thickness, head to medium separation and a recording constant (a computed plot of equation 38 is given in Fig. 21). And another expression for the head output voltage, for the signal array using NRZ recording, and described by equation (49) was given by the equation (54) using harmonic analysis. A detailed analysis of the playback process limitations from these deductions will not be attempted here to keep the size of the paper within a reasonable limit, only the salient features will be stated. Theoretical and experimental findings on pulse width and amplitude as a function of separation between P.B. head and layer surface agree well, and the difference may be attributed to the self-demagnetization and record head trailing effects which are dependent on coating thickness.

Effect of p.b. head gap width.

It can be stated from physical reasonings that the sensitivity contour of the P.B. head should be wide and sharply defined enough to be able to intercept as much flux as is possible during reading operation from the recorded spots. The total flux intercepted by the head will be

$$\phi_x = \int_{x-\omega/2}^{x+\omega/2} \phi_x dx$$

Therefore,

$$e_x = K \frac{d}{dx} \int_{x-\omega/2}^{x+\omega/2} \phi_x dx \qquad \dots \quad (67)$$

where K is proportionality constant involving number of turns in the head, surface speed and all other variables including ω. (ω = width of the P.B. head sensitivity contour). Using the formula of Leibuitz, (67) becomes

$$e_x = K[\phi_{x+\omega/2} - \phi_{x-\omega/2}] \qquad \dots \quad (68)$$

The maximum signal amplitude is

$$e_{max} = e_0 = K[\phi_{\omega/2} - \phi_{-\omega/2}]$$

But $\qquad \phi_{\omega/2} = \phi_{-\omega/2}, \therefore e_{max} = 2K\phi_{\omega/2}.$

For pulse width at N per cent of the peak amplitude the following equation must hold

$$0.02N\phi_{\omega/2} = \phi_{x_N+\omega/2} - \phi_{x_N-\omega/2} \qquad \dots \quad (69)$$

x_N is the head position where the amplitude has dropped to N per cent of the peak value. The solution for $2x_N$ will give pulse width as a function of gap width.

But the above equation can not be solved directly as ϕ is a transcendental function. The equation can be solved graphically for particular systems. One point should be marked here is that the effective gap width is not necessarily the physical gap width. And the effective gap width is to be determined, by measuring the wavelength where the 1st minima in signal occurred (Bagun, 1955). So if the pulse width is not to exceed certain limit of an absolute minimum, the effective gap width for the system can be determined. In general, it would be desirable to use the largest gap width consistent with satisfactory performance.

CONCLUSIONS

A comprehensive theoretical and experimental investigation on digital data recording and reproduction on and from ferromagnetic layer surface of magnetic drum memory has been presented. The boundary value problem has been solved to find the distribution of the fringing field in the ferromagnetic layer surface. Analytic expressions for the output of a Write-Read system employing saturation recording on a magnetic medium in terms of the basic system parameters have been presented.

The variables involved in the process of pulse recording on a moving magnetic surface and their influences were experimentally studied with a practical magnetic drum storage system, which has special features for studying the influence of different parameters.

Both theoretical and experimental investigations, and physical analysis of the factors involved in the process lead to the conclusion that the following are the basic requirements for achieving high resolution pulse recording on magnetic surface :

1) Recording pole face configuration for having maximum flux gradient on the surface for a particular head to medium separation.

2) Rectangular B-H loop characteristics of the coating material to reduce the record head trailing effect and the self-demagnetization effect.

3) High ratio of H_s to B_r to reduce the self-demagnetization effect.

4) Optimum recording current.

5) Minimum coating thickness consistent with satisfactory operation to reduce the record head trailing effect, self-demagnetization effect, and loss of resolution in the P.B. process.

6) Minimum head to coating separation to reduce record head trailing effect and loss of resolution in the P.B. process.

7) Largest effective gap width which will give required resolution for the particular coating, record head and head to coating separation so that tolerances involved in the construction of the head can be relaxed and the performance characteristics made more uniform.

6

REFERENCES

Begun S. J., 1949, "Magnetic Recording, Murray Hill Books Inc.
Bigelow, J. H. and others, 1948, "First Progress Report.... I.A.S. Princeton.
Booth, A. D., 1949, July, *Electronic Engineering.*
Booth, A. D., 1952, *Brit. Jour. Appl. Phys.*, 3.
Bozorth, R. M., 1951, "Ferromagnetism   pp. 351-53.
Byerly, W. E., "Fourier s Series and Sphcyl. and Ellips Harmonics, Grinn and Company.
Dutta Majumdar D., 1958, *Electronic Engineering,* 702-5.
      „   „   „   1959, *J. Inst. Telecomm. Engrs.,* 5, 4, 211-22.
Dutta Majumdar D., 1961, *Proc. Ind.* Sc. Congress, Roorki, Session.
      „   „   „   1961, *J. Inst. Telecomm. Engrs.,* 7, 1, 27-36 ;
      „   „   „   and Biswas, R. 1962 (Communicated) I.G.P.
Evershed, E., 1958, *J.I.E.E.,*
Karlqvist, O., 1954, *T. R. I. T.,* Sweden.
Kostyshyn, B., 1961, *IRE Conv. Proceedings.*
Kostyshyn, B., Roshon, D., 1959, *Proc. IRE.,* 47, 451.
Wallace, R. L., Jr., 1951, *B. S. T. J.,* 30, 1146-73.
Westmijze, W. K., 1953, Philips Research Report, Vol. 8.